

# Density Limit Disruption Induced by Core-localized Alfvénic Ion Temperature Gradient Instabilities in HL-2A NBI Plasmas

W. Chen<sup>1</sup>, L. W. Hu<sup>1</sup>, J.Q. Xu<sup>1</sup>, R.R. Ma<sup>1</sup>, P.W. Shi<sup>1</sup>, R. Ke<sup>1</sup>, H.T. Chen<sup>1</sup>, X.X. He<sup>1</sup>, Y.G. Li<sup>1</sup>, L.M. Yu<sup>1</sup>, W.P. Guo<sup>1</sup>, M. Jiang<sup>1</sup>, J.M. Gao<sup>1</sup>, X. Yu<sup>1</sup>, Z.J. Li<sup>1</sup>, H.L. Wei<sup>1</sup>, and Z.B. Shi<sup>1</sup>

<sup>1</sup> *Southwestern Institute of Physics, P.O. Box 432 Chengdu 610041, China*

Density limit experiments were conducted on the HL-2A tokamak. The experimental campaign involved systematic scanning of plasma density under controlled conditions, utilizing neutral beam injection (NBI) heating scenarios. Fig.1 presents a high-density disruption event during low-power NBI heating (ShotNo.38600). The magnetic probe signals exhibit characteristic rapid changes preceding the disruption at  $t = 1578$  ms. Before the disruption, the plasma density approaches the Greenwald density with  $ne/ne_G \sim 1.0$ . The plasma parameter evolution reveals the interplay between plasma heating, density evolution, radiation and stability limits. Fig.2 illustrates the temporal evolution of plasma instabilities in this discharge, combining measurements of the density profile and core microwave interferometer spectrogram. The observed instabilities are unstable during  $t = 1525 - 1578$  ms. These instabilities are rarely observed in the Mirnov signals. These instabilities, characterized by poloidal ( $m$ ) and toroidal ( $n$ ) mode numbers, can exhibit complex frequency dynamics including multiple spectral bands, mode coexistence, abrupt frequency jumps, and stair-like frequency progression[1]. These instability characteristics are determined by the following specialized diagnostics. The magnetic pickup probes exclusively measured low-frequency (LF) modes with toroidal mode numbers  $n = 2 - 4$ . The core beam emission spectroscopy (BES) solely detected LF modes with poloidal mode numbers  $m = 4 - 10$ . The core microwave interferometer provided an optimal response exclusively for frequencies in the  $0 - 500$  kHz range. Notably, these diagnostic techniques can resolve only low mode numbers, whereas the higher mode numbers are derived from low mode number measurements and Doppler frequency shift induced by the plasma toroidal rotation. The  $m/n = 2/1$  instability is localized at the  $q = 2$  rational surface, while the high- $n$  instabilities are localized at the  $q = m/n \sim 1$  surface. As the plasma density increases, these instabilities evolve from high- $n$  to low- $n$  modes while propagating from the core toward the edge.

Fig.3 presents the kinetic instability evolution in HL-2A (ShotNo.38546) following NBI switch-off in the high-density regime. These observed instabilities display complex temporal evolution patterns that vary systematically with plasma parameters and heating conditions. The observed frequency structures provide valuable signatures for real-time disruption prediction systems. These instabilities are not observed during NBI heating due to the low plasma den-

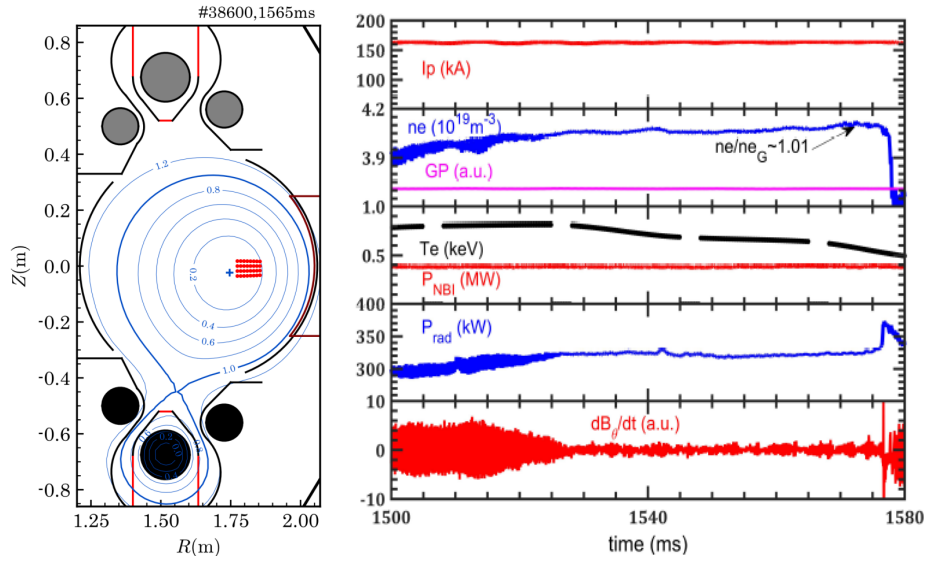


Figure 1: A typical high-density disruption discharge with low-power NBI heating on HL-2A (ShotNo.38600). Plasma poloidal flux surface at  $t = 1565$  ms, and the red dots show the locations of the core beam emission spectroscopy (Left col.). From top to bottom: plasma current ( $I_p$ ), line averaged electron density ( $ne$ ), standard gas puffing ( $GP$ ), core electron temperature from TS ( $Te$ ), NBI heating power ( $P_{NBI}$ ), total radiation power ( $P_{rad}$ ), and magnetic probe signals ( $dB_\theta/dt$ ) (Right col.).

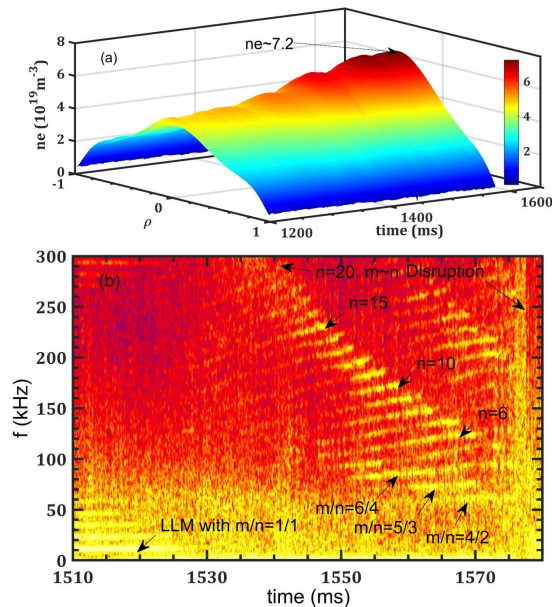


Figure 2: Time evolution of the plasma density profile (a) and spectrogram of the core microwave interferometer signal (b) (ShotNo.38600). The LLM in the figure denotes the long-lived mode instability, with  $m$  and  $n$  being the poloidal and toroidal mode numbers of the instability, respectively. The observed instabilities during  $t = 1525 - 1578$  ms exhibit the distinct frequency dynamics, such as multiple bands, mode coexistence, frequency jumps and stair-like patterns.

sity, but emerge after NBI heating as the plasma density increased. Since their excitation does not depend on NBI heating, these instabilities are driven unstable by energetic-ions. Remarkably, identical instabilities have also been observed in HL-2A pure Ohmic high-density plasmas. Following NBI switch-off, these instabilities exhibit distinctive frequency dynamics including mode coexistence and structures resembling Christmas lights or mountain peaks[1, 2]. These patterns reflect the complex nonlinear interactions between different mode structures and their coupling with background plasma profiles. These instabilities precede the disruption by  $\delta t = (1892 - 1817) \text{ ms} = 75 \text{ ms}$ , therefore, it can be concluded that these instabilities reveal characteristic behaviors that serve as important signatures for disruption prediction.

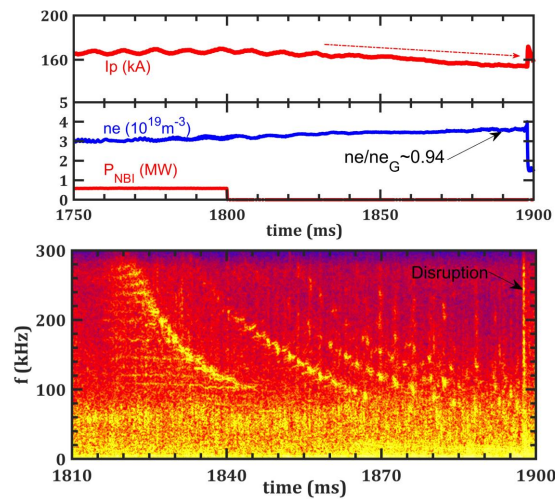


Figure 3: Time evolution of kinetic instabilities in high-density regime after NBI switched-off on HL-2A (ShotNo.38546). From top to bottom: plasma current ( $I_p$ ), line averaged electron density ( $ne$ ), NBI heating power ( $P_{NBI}$ ), and spectrogram of the core microwave interferometer signal. The instabilities exhibit the distinct frequency dynamics, such as mode coexistence and structures resembling Christmas lights or mountain peaks.

These measured instabilities have been identified as AITG modes by the gyrokinetic code GENE[3]. Fig.4(a-b) present the plasma profiles including the temperatures, density, toroidal rotation frequency and safety factor. Fig.4(c-d) are the linear eigenvalue spectrums at four radial positions. These modes are identified as AITGs, which can be inferred from their large positive real frequencies, as shown in Fig.4d. Considering the plasma toroidal rotation frequency, the simulated mode frequency shows good agreement with experimental measurements. The physical mechanism is that the magnetic shear is relatively small at the diagnostic positions hence these electromagnetic modes can be excited easily, which are further destabilized when moving outward as the gradients becomes larger. The simulations revealed that low and

medium wavenumber modes become unstable across multiple radial positions, with instability growth increasing from inner to outer regions due to strengthening plasma gradients, as shown in Fig.4c. This radial dependence provides important insights into the instability drive mechanisms and their relationship with plasma parameters.

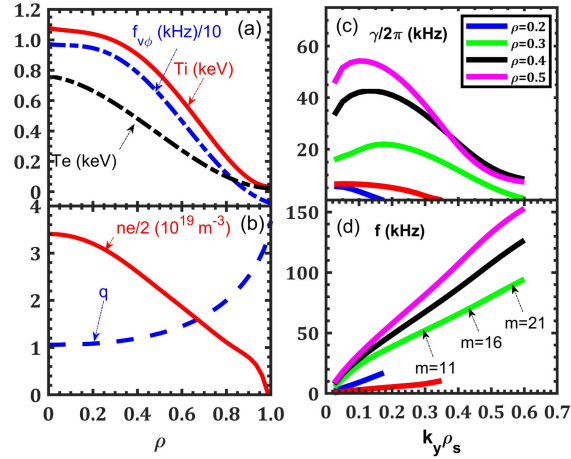


Figure 4: Plasma profiles (a-b), showing the electron temperature ( $T_e$ ), ion temperature ( $T_i$ ), toroidal rotation frequency ( $f_{v\phi}$ ), electron density ( $ne$ ), and safety factor ( $q$ ), respectively (Shot-No.38600,  $t=1537$  ms). Dependence of instability growth rates (c) and real frequencies (d) on wave-numbers ( $k_y \rho_s$ ) at different radial positions ( $\rho$ ), as given by GENE code.

We present the recent experimental results of the density limit disruption and core-localized kinetic MHD instabilities in HL-2A NBI plasmas. It is discovered for the first time that there are multiple branch MHD instabilities in the core plasmas while  $n_e/n_{eG} > 0.85$ . The analysis suggests that the core localized (from  $\rho_{q=1}$  to  $\rho_{q=2}$ ) MHD activities belong to AITG modes, and it is found, for the first time, in experiment that they trigger the disruption of bulk plasmas while the density is peaked. These AITG instabilities hold promise as artificial intelligence (AI) predictors for real time disruption forecasting in future tokamak fusion reactors, with predictive lead times of tens of milliseconds. Our findings establish a new physical picture that fundamentally challenges the conventional edge-centric paradigm for density limit disruptions. The identification of core localized AITG instabilities as triggers of disruptive events marks a significant advance in understanding plasma stability boundaries in toroidal confinement systems.

## References

- [1] Chen. W. *et al. EPL* **116**, 45003(2016).
- [2] Heidbrink. W. W. *et al. Nucl. Fusion* **61**, 016029 (2021).
- [3] Jenko. F. *et al. Phys. Plasmas* **7**, 1904(2000).